Egypt. J. Geo. **Vol. 68,** pp: 177-197 (2024)

Egyptian Journal of Geology

https://egjg.journals.ekb.eg

Petrology and geochemistry of some Egyptian granitic rocks: Evaluation of physical and mechanical properties of the granites used as construction materials

Ahmed M. Arafat[1*], Hatem Mohamed El-Desoky[1], Nabil A. Abd Alhafz[1] and **Ahmed E. Khalil[2]**

[(1)] Geology Department, Faculty of Science, Al-Azhar University, PO Box 11884, Nasr City, Cairo, Egypt

[(2)] Department of Geological Sciences, National Research Center, Dokki Cairo, Egypt

THE CURRENT study deals with the field geology, petrography, and geochemistry of some Egyptian granitic rocks and its suitability for construction materials. Also, the present work aims to determine the physical and mechanical properties of some granites in the northeastern Desert of Egypt to detect their suitability for ornamental stones. Granitic rocks are regarded as one of the most significant commercial commodities and are utilized for a variety of uses, including as decorative stones. The main applied tests of physical and mechanical properties include compressive strength, apparent porosity, specific gravity, water absorption, abrasion resistance, thermal expansion, weather and frost resistance, and acidic resistance. The study district geologically is forming moderately high mountainous ridges with hard topography and curly peaks. The collected sample petrographically divided into biotite monzogranites, alkali feldspar granites, and riebeckite- arfvedsonite granites (peralkaline granites). Meanwhile, the chemical classification of these granites was distributed between the granite, granodiorite, syenodiorite, monzogranite, syenite, and alkali granite fields and all the studied samples have alkaline to peralkaline affinity and metaluminous to peraluminous nature and also classified as I-type orogenic granites and A-type anorogenic granites. The studied samples were cut according to the American Society for Testing and Materials specifications (cubic shape) for detection the physical and mechanical properties. The compressive strength ranges from 795 to 979 kg/cm^2, apparent porosity ranges from 0.35% to 0.58%, specific gravity ranges from 2.67 to 2.79 gm/cm^3, water absorption ranges from 0.13% to 0.22%, abrasion resistance is good, thermal expansion ranges from 0.02 to 0.06, weather and frost resistance are good, and acidic resistance are good. It should be noted that the studied granitic samples showed good results according to mechanical and physical tests. So that it can be used in decoration purposes and construction materials

Keywords: Ornamental stones, petrography, geochemical characterization, mechanical and physical properties.

1. Introduction

The natural stones are the most common materials extracted from the earth rocks and used for construction, accommodation, and artistic purposes. Stones have allowed us to build durable structures, solid works of art, arches, bridges, and inns. The natural stones were used for construction purposes and building materials because they contain hard and massive minerals. Today, these natural building stones are used for aesthetic purposes in modern architecture and for different purposes (interior and exterior decoration, paving, siding, etc.).

Granite rocks is intrusive igneous rock composed of quartz and feldspars which exhibits different textures and has medium to coarse grains. Due to its high compressive strength, it has been widely used in the construction industry, and being the signature earth rock, deep mining operations are often conducted in the granitic rocks. Granitic rocks have been used as building materials from ancient times, it is a granular igneous rock with visible granules that variety in color which increasing its economic value. It is one of the very oldest and most long-lasting building products available on the earth

*Corresponding author e-mail: arafatahmed048@gmail.com
Received: 22/06/2024; Accepted: 29/04/2024
DOI: 10.21608/EGJG.2024.298345.1080

surface. Because of its durability and variety of textures, it has become the first material of choice for using as ornamental stone. The primary mechanical and physical characteristics of granite allow it to satisfy the requirements of a wide range of construction applications, especially in the decorative finishing stages of pavement, bridges, and structures. Granite is one of the hardest, compacted, and most dense types of igneous plutonic rocks. They are sought-after as ornamental components in artwork and architecture because of their exquisite hues, patterns, and sheen. Previously, nearly eighty-four different types of decorative stones were used by the ancient Egyptians, 45 of which were from well-known and well-liked archeological quarries. (Harrell, 2013). Preserving the entire local legacy begins with recognizing and utilizing the resources found in historical and rural structures. (Dino et al., 2015).

Granites are created by the cooling and solidification of the granitic magma at deeper levels of the earth. Chemically, granite is rich in silica (SiO2) and alumina (Al2O3). Since the granites form at greater depths, they cool slowly and thus, medium to coarse grains are formed. It is the oldest and one of the hardest rocks (Agasnalli et al., 2022). The features of this batholith are consistent with it being an entirely intrusive igneous body and not as an autochthonous discovery of granitoid from the Pan-African Remobilized basement rocks as proposed by Akaad et al. (1973), El-Gaby and Habib (1982), Habib (1987), El-Gaby (1990) and El-Bialy and Omar (2015). Significantly the ornamental stones are represented by specific, igneous, metamorphic, and sedimentary rocks distinguished by high strength, hardness, and resisting climate changes, preserving their varied wonderful colors and patterns (Bates, 1969 and Brown, 2015). They are widespread in Egypt and representing the Nile Valley, Sinai, and the Eastern Desert. The investigated granites have normal radioactivity concentrations (Awad et al., 2022), so they can be used economically in the field of construction, decoration, and other economic purposes (Fig.1).

1.2 Geologic setting

The topography of the studied granites ranges from medium to high mountainous terrain. It includes distinguished mountains such as Gabal Risays, Gabal Ghuwayrib, and Gabal Gharib (Fig. 2). The study region is traversed by a number of wadis flowing north-east towards the Gulf of Suez, such as Wadi Faliq El-Wa`ar, Wadi El-Ghafiryia, and Wadi Al-Ushsh. They consist of varicolored relay successions of granitic rocks.

The study district is bounded by latitudes 27° 00' 00" to 28° 12' 00"N and longitudes 32° 42' 45" to 33° 48' 00"E and forming moderately high mountainous ridges with hard topography and curly peaks (Fig.3a-e). The Egyptian granitic rock has been differentiated into two broad categories; namely syn- to late-orogenic granitoids (685-610 Ma; Stern and Hedge, 1985) and post-orogenic to anorogenic granites (600–475 Ma; Stern and Gottfried, 1986; Willis et al., 1988; Moghazi, 2003 and Jarrar et al., 2003). They previously identified as older granitoids and younger granites (El-Ramly, 1972 and Noweir et al., 1990). Approximately 27% of the basement rocks in the Eastern Desert is made up of older granitoids basement outcrops (Stern, 1979) and compositionally ranges from quartz diorite to granite (predominantly trondhjemites, tonalites, and granodiorites). They were emplaced during the main orogenic stage between 800 and 614 Ma ago (Stern and Hedge, 1985 and Hassan and Hashad, 1990; Shahin, 2023). The younger granites constitute approximately 30% of the Egyptian plutonic assemblages (Hassan and Hashad, 1990). The studied granites are represented by late-orogenic granites (Monzogranites and alkali feldspar granites) and post-orogenic granites (Peralkaline granites). The studied granitic rocks are crosscut by numerous post-orogenic dykes of basic composition. These basic dykes are most abundant and widespread in the regions comprising basalts and basaltic andesites (Fig.4b, c, d & e). The dykes are extending in dominant NE, NNE, and ENE trends. The dykes are mostly straight reveals that they have been apparently emplaced along sharply defined fractures.

Monzogranites are buff in color, medium to coarse-grained and characterized by low to moderate relief, jointed, bouldery weathering, and spheroidal exfoliation exposed at Wadi Falig El-Wa`ar (Fig. 4a). Offshoots and apophyses of Wadi El-Ghafiryia monzogranites was extruded by basaltic dykes (Porphyritic with K-feldspar megacrysts; Fig.4b). These El-Ghafiryia monzogranites have yellowish pink color and form small intrusions. Wadi Al-Ushsh monzogranites present as massive, reddish white, buff in color, and dissected by basic dykes (Fig. 4c). Gabal Risays alkali feldspar granites form massive to weakly deformed elongated bodies with moderate to high relief, and extruded by the younger volcanic dykes (Fig.4d & e). Post-orogenic granite occurs as massive, grey, whitish pink, and medium- to coarse-grained (Fig.4f). Gabal Gharib (1,751 m) high relief covers an area of about 25 km2 with oval to circular outlines and composed of peralkaline granites (Fig.4f).

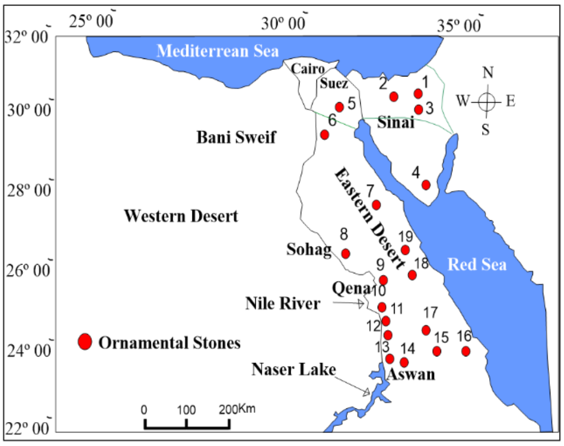

Fig. 1. A location map displays the granitic rocks distribution across Egypt's many locales. (Ciccu et al., 2005).

2. Materials and Methods

A total of 15 rock blocks of granites Stones were gathered and examined for this study and which were sufficiently big and uniform to offer test specimens devoid of fractures, joints, or partings. Then crushed and powdered by using a stainless-steel jaw crusher and an agate ball mill machine at the laboratories of the National Research Center of Egypt (NRC). the petrography and geochemical characteristics were identified. The chemical composition of major oxides and trace elements were determined in the studied granitic samples by using the X-ray fluorescence spectrometer (Model: A Philips Pw/2404, 30 kV), available at the Housing and Building National Research Center (HBRC), Cairo, Egypt. Standard petrographic thin sections were prepared and examined to analyze the microfabrics, identify the granitic samples, mineralogical composition as well as the structure and texture. The ornamental stone samples were prepared according to the American Society for Testing and Materials specifications (cubic shape). The studied samples were cut as 50x50x50 mm. The samples were tested by using a calibrated and certified 1500 KN compression testing machine.

3. Result and Discussion

3.1 Petrography

3.1.1 Biotite monzogranites

Monzogranites are coarse-grained rocks, exhibit equigranular hypidiomorphic, micrographic, and perthitic textures. They are mainly composed essentially of quartz, perthite, plagioclase, potash feldspar (Microcline and orthoclase), and biotite (Fig.5a, b, c & d). Opaques, allanite, zircon, apatite, and titanite are accessories. Chlorite, kaolinite, and sericite occur as secondary alteration minerals.

Plagioclase represented by euhedral and subhedral elongate and tabular crystals deformed, cracked, and observed showing zonation, Manebach twinning partially altered to sericite (Fig.5a). Quartz occurs in two generation the first is the primary quartz and present as coarse-grained exhibit undulose extinction and the second is the fine-grained and occurs as secondary quartz due to silicification. Quartz is represented by subhedral to euhedral crystals (Fig.5b).

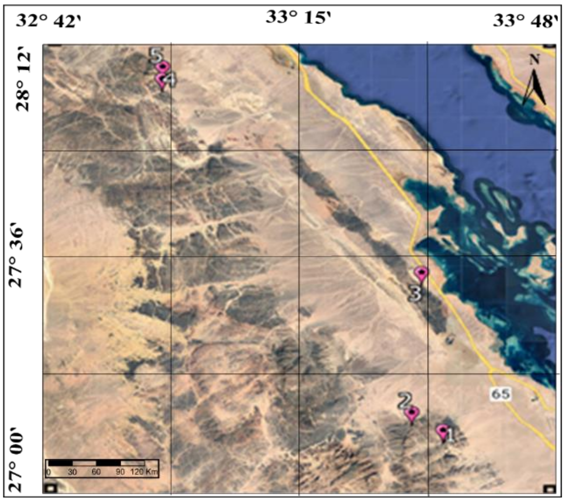

Fig 2. Landsat image showing the location of the studied granitic rock regions encountered in Egypt: 1. Faliq El-Wa`ar, 2. Wadi El-Ghafiryia, 3. Wadi Al-Ushsh, 4. Gabal Risays, 5. Gabal Gharib.

Mica minerals in the studied monzogranites are biotite. Biotite occurs as anhedral to subhedral flakes that enclose fine zircon prisms. Biotite occurs as yellowish-brown flaky crystals. It is pleochroic from yellowish brown to pale yellow to brown color. It is corroded and replaced by groundmass altered to chlorite (Fig.5c & d). Orthoclase perthite occur as medium grained euhedral crystals. Generally, it is characterized by simple twinning and exhibits perthitic texture as result to intergrown between plagioclase and K-feldspars (Fig.5e & f). Potash feldspar altered to secondary alteration minerals such as sericite and kaolinite (Fig.5c & d).

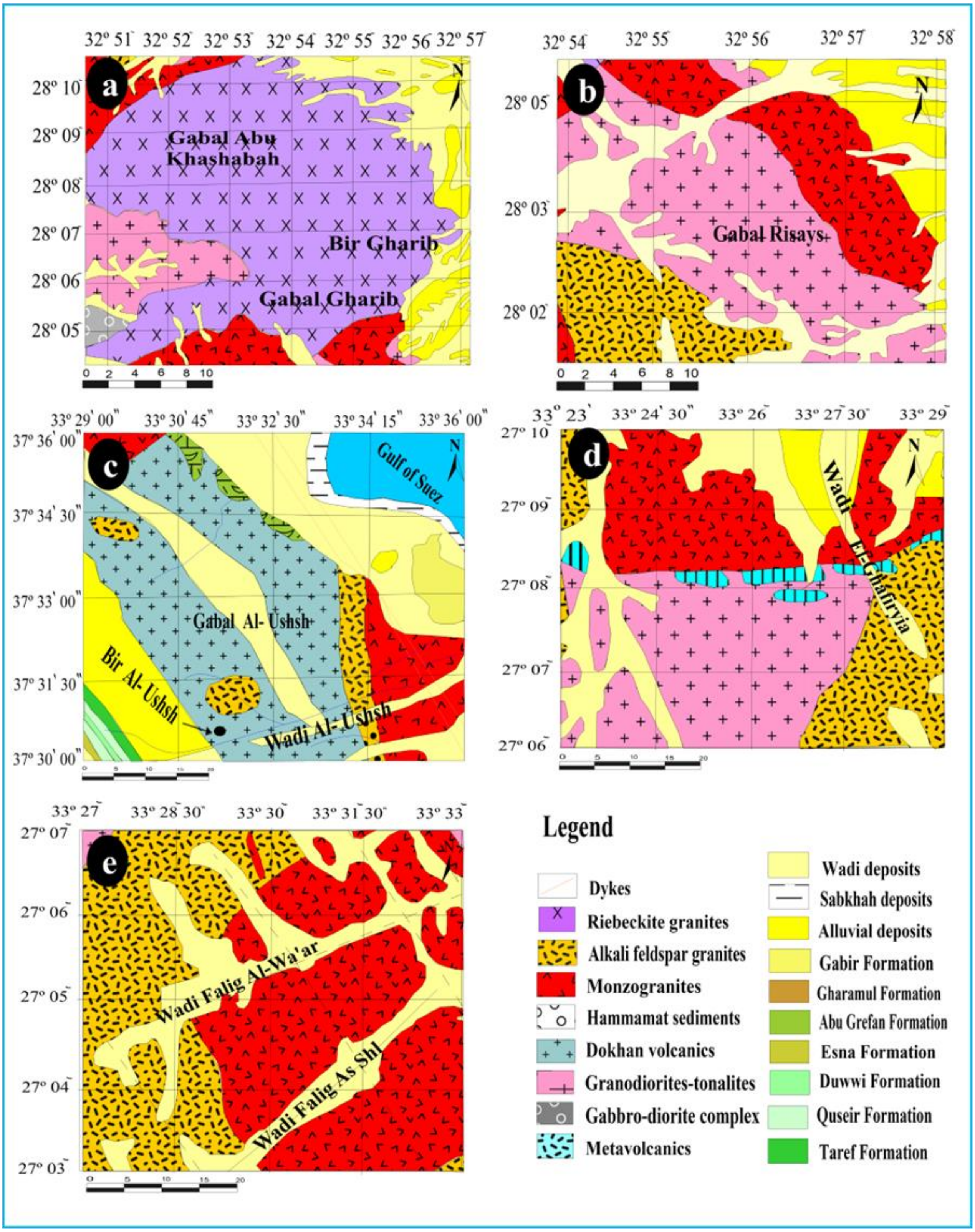

Fig. 3 (a-e). Geological maps of the study regions (El-Desoky et al., 2023).

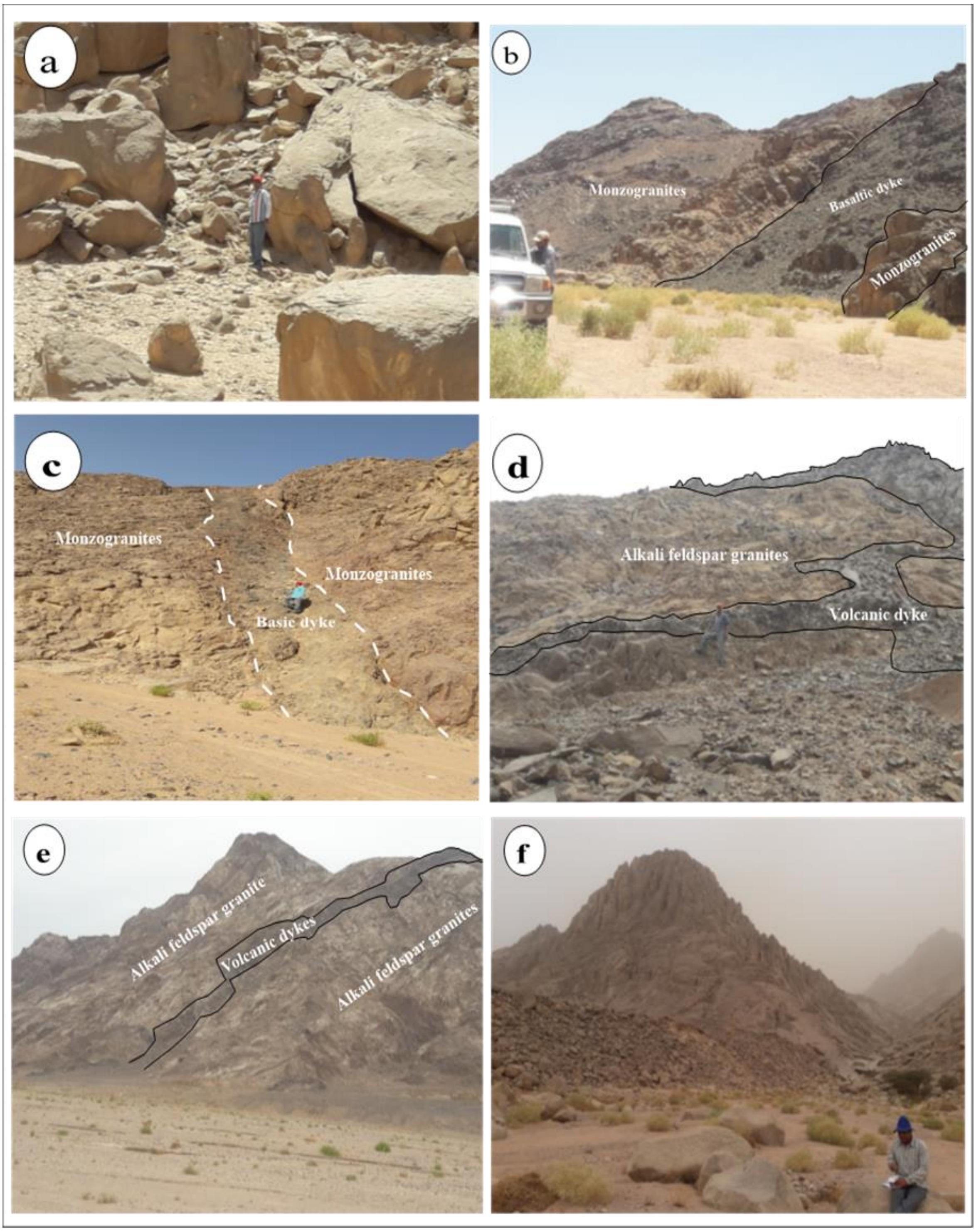

Fig. 4 (a-f). Field photographs showing the observations of the sudied granites.
a. Jointed and exfoliated monzogranites exposed at Wadi Falig El-Wa`ar (Looking S-E).
b. El-Ghafiryia monzogranites were extruded by basaltic dykes (Looking S-E).
c. Massive, reddish to buff monzogranites extruded by basic dykes exposed at Wadi Al-Ushsh (Looking N-W).
d & e. Alkali feldspar granites extruded by younger volcanic dykes at Gabal Risays (Looking S-E).
f. High relief Gabal Gharib post-orogenic granites are greyish pink, medium- to coarse-grained (Looking N-W).

3.1.2 Alkali feldspar granites

Alkali feldspar granites consist essentially of quartz, potash feldspars, plagioclase, and orthoclase perthite crystals. They are medium- to coarse-grained, euhedral to subhedral crystals and showing often perthitic texture. Biotite is less common and altered to chlorite. Opaque minerals, allanite, and titanite are the chief accessory minerals. Chlorite and sericite are the main secondary minerals. Quartz is filling the interstitial spaces to the other mineral constituents and showing strong undulose extinction (Fig.6a), it founds as medium- to coarse-grained, anhedral to subhedral large crystals. Alkali feldspars occur as subhedral tabular crystals constitute essentially from orthoclase perthites in both monzogranites and alkali feldspar granites. Generally, perthites are of flame, string, and patchy types (Fig.6b). Perthites are abundant up to 55% of the total constituents and represented by orthoclase and microcline perthites. They occur as subhedral crystals and are highly altered to sericite flakes (Fig.6b). Plagioclase The composition of plagioclase in monzogranites and alkali feldspar granites has anorthite contents of (An14–20 and An5–10), respectively. Plagioclase is mainly albite in composition with an anorthite content is represented by subhedral tabular crystals, it shows albite twinning and altered to sericite. Occasionally, plagioclase crystals are intergrown with the potash feldspars forming perthitic texture (Fig.6b & c). Biotite is subordinate mineral and occurs as subhedral flaky or platy crystals with inclusions of opaque minerals and intensely altered to chlorite (Fig.6d).

3.1.3 Riebeckite - arfvedsonite granites (Peralkaline granites)

The granite is composed mainly of alkali feldspars with interstitial quartz, arfvedsonite, and riebeckite. Alkali feldspars are represented by microcline, orthoclase, microcline-perthite, and orthoclase-perthite. All of them are varying from subhedral to anhedral shapes. Sometimes, they are slightly corroded. Given that quartz and arfvedsonite are interstitial to alkali feldspar, it was the first necessary mineral to crystallize. It is primarily represented by perthite, which makes up to 60% of the rock and is followed in importance by albite. These granites are medium-grained and consist essentially of K-feldspars, albite, alkali amphiboles including riebeckite and arfvedsonite, subordinate amounts of biotite and quartz. Zircon, apatite, allanite, and opaque minerals are the common accessories.

Quartz occurs as subhedral and euhedral crystals scattering over all the mineral constituents, showing usually undulose extinction (Fig.7a). Quartz present as subhedral crystals aggregates. Zircon, ilmenite, and K-feldspar are included in it. Between perthite grains is a thin ring of secondary albite that is dentate and untwined. Orthoclase perthite occurs often mantled by narrow rims of sodic plagioclase and showing quite lamellar twinning. These perthites are mainly represented by string, flaky and vein types (Fig.7b). Plagioclase is mainly albite with anorthite content. It occurs as subhedral and euhedral crystals showing often albite-lamellar sometimes their lamellar twinning disappear (Fig.7c) as well as it occurs surrounding other K-feldspar crystals to form rapakivi texture. Biotite is represented by prismatic crystals it is corroded and partially to totally altered to chlorite (Fig.7d). Titanite is represented by sphenoid shape, high relief pleochroic from yellowish brown to brown color (Fig.7d). Opaque and allanite minerals occur as accessory minerals fine-grained scattered on the other minerals (Fig.7d). Riebeckite Only in alkali feldspar granites can one witness riebeckite, which occurs as anhedral to subhedral crystals that surround zircon, opaques, and allanite inclusions and are extremely pleochroic from green to blue green. (Fig.7e). Riebeckite occurs as brownish green in color and medium to coarse-grained (Fig.7e). Arfvedsonite is present as large plates up to 5 mm long or as smaller acicular crystals interstitial between alkali feldspar. Two sets of cleavage are characteristic, and the color varies from pale to dark green. Arfvedsonite also occur as anhedral to subhedral crystals with pleochroism from green to pale green to brown (Fig.7f). Sometimes, it is corroded and speckled with iron oxides and altered to chlorite. Alkali feldspar, quartz, fluorite, apatite, zircon, and ilmenite with other unidentified minerals are the main inclusions observed in the arfvedsonite plates. The arfvedsonite plates are locally altered to chlorite, titaniferous biotite, and hematite. Zircon is present as short prisms included in the main constituents.

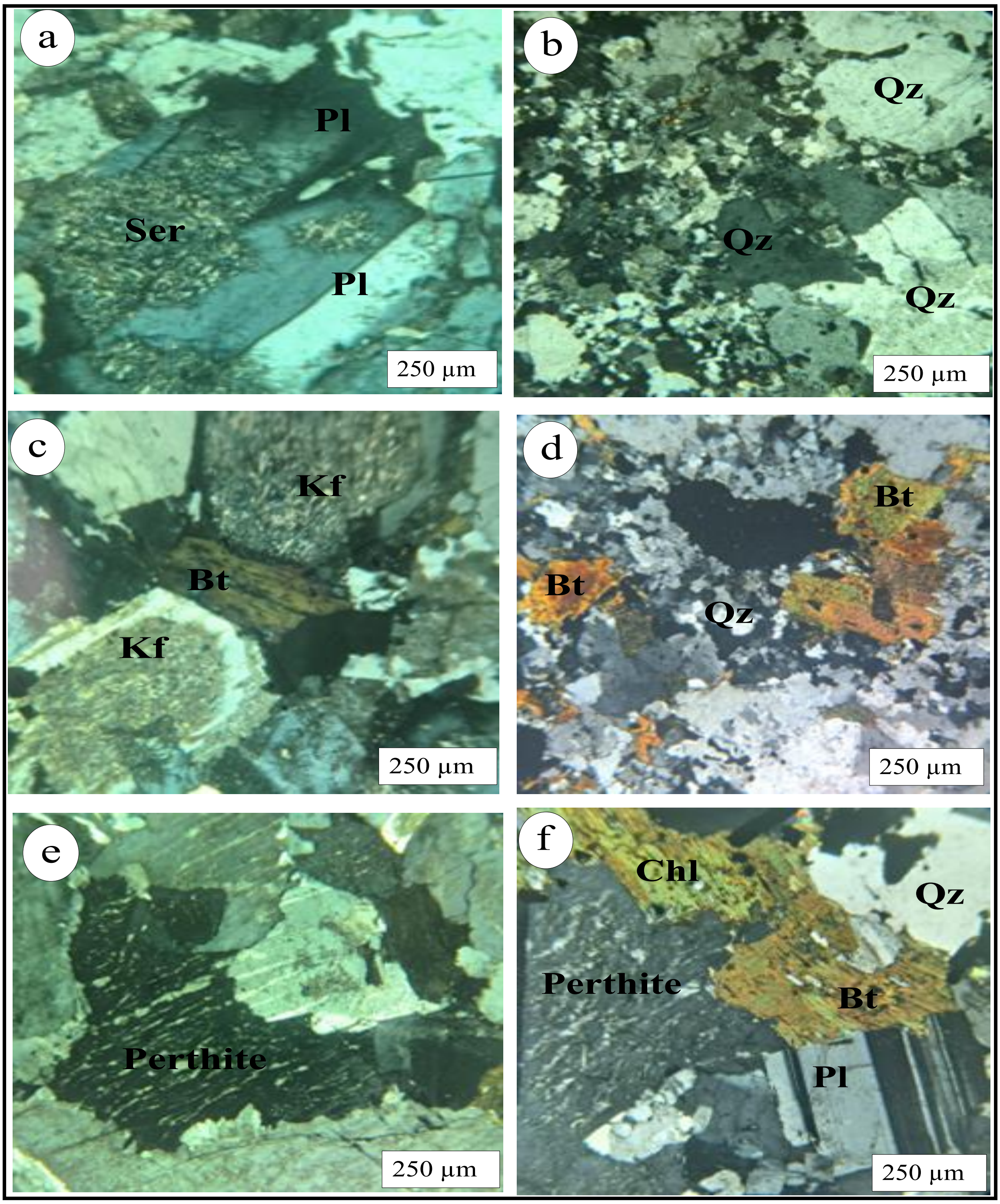

Fig. 5 (a-f). Photomicrographs showing the main petrographic features for the studied biotite monzogranites.
a. Plagioclase crystals exhibit Carlsbad twinning and partially altered to sericite (Ser; CN).
b. Anhedral quartz crystals (Qz) occur as fine and coarse grains (CN).
c. K-feldspar highly altered to sericite and kaolinite (CN).
d. Biotite crystals (Bt) crystal partially altered to chlorite associated with fine-grained quartz (Qz; CN).
e. Medium- to coarse-grained of perthite crystals (CN).
f. Biotite crystal partially altered to chlorite (Chl) and opaque minerals with well-developed perthite, quartz (Qz), and plagioclase crystals (Pl; CN).

Fig. 6 (a-f). Photomicrographs showing the main petrographic features of the studied alkali feldspar granites.
a. Anhedral to subhedral quartz crystals found as medium- to coarse-grained (Qz; CN).
b. Perthites are of flame and patchy types (CN).
c. Plagioclase with albite twinning partially altered to sericite (Ser; CN).
d. Subhedral flaky and platy biotite crystals and intensely altered to chlorite crystals (CN).

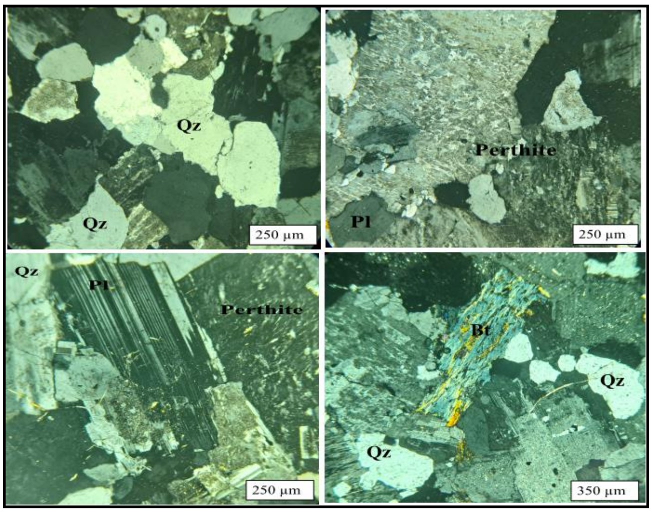

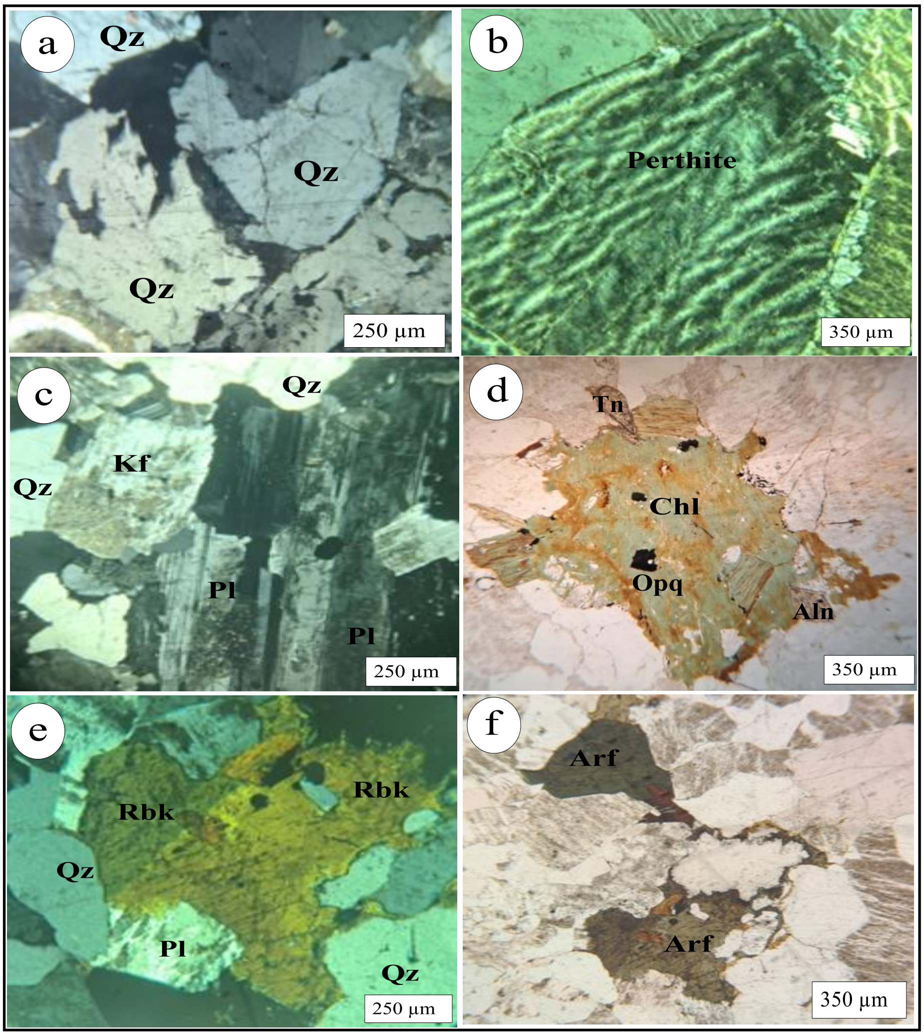

Fig 7 (a-f). Photomicrographs showing petrographic feature of the studied riebeckite- arfvedsonite granites.
a. Subhedral and euhedral quartz (Qz) crystals aggregate usually showing undulose extinction (CN).
b. Perthites present as string, flaky, and vein types (CN).
c. Subhedral tabular plagioclase crystals showing albite-lamellar twinning (CN).
d. Biotite crystals intensely altered to chlorite (Chl) associated with opaques, allanite (Aln), and titanite (Tn; PPL).
e. Subhedral riebeckite crystals (Rbk), strongly pleochroic from green to bluish green in color (CN).
f. High relief anhedral arfvedsonite crystals interstitial between the alkali feldspars (PPL).

3.2 Geochemical characterization

Twenty granitic samples of biotite monzogranites, alkali feldspar granites, and riebeckite- arfvedsonite granites (peralkaline granites) were examined for trace elements and major oxides in order to determine the geochemical characteristics. The analyzed samples had been done in the laboratories of National Research Center (NRC), Egypt (Table 1).

The compositions of granitic rocks exhibit wide range of silica (SiO_2) saturation from (62.61) to (73.20 %) with an average (68.41%). Silica content decrease at Wadi Al-Ushsh granites refer to that it is biotite monzogranites affected by desilicification hydrothermal alteration.

The Harker variation diagrams display the chemical variations and trends among the related rock varieties (Figs.8 & 9). Within such variation diagrams, the plot of SiO_2 against major oxides and trace elements (Figs.8 & 9) discriminate two distinct geochemical trends, corresponding to the physicochemical processes that operated in the magmatic crystallization. The studied granites plot of SiO_2 against TiO_2, Al_2O_3, FeO, Fe_2O_3, MnO, MgO, CaO, P_2O_5, Zn, Ba, and Sr demonstrate the reversible relationships between SiO_2 and these oxides (Figs.8 & 9). Meanwhile, the SiO_2 versus Na_2O, K_2O, Rb, Ga, Pb, Zr, and Y exhibits the irreversible relationship(s) between these oxides and SiO_2 contents.

The studied granitic rocks are classified by using several diagrams based on different geochemical parameters. Cox et al. (1979) used the relation between (Na_2O+K_2O) and SiO_2 as well as also Hunter et al. (1978) used the relationship(s) between the CaO - Na_2O - K_2O oxides to classify the plutonic igneous rocks. The plots of analyzed granitic samples on these diagrams are fall within the granite, granodiorite, syenodiorite, monzonite, syenite, and alkali granite fields (Fig.10a & b).

The magma type of the investigated granitic rocks is discussed on the base of the following proposed diagrams. ANK versus ACNK variation diagram of Maniar and Piccoli (1989) shows wide variation of the examined biotite monzogranite and alkali feldspar granite samples, where they are laying on the field of metaluminous to peraluminous orogenic granites. On the other hand, the riebeckite- arfvedsonite granite samples are located on and nearby the fields of the metaluminous - peralkaline anorogenic granites (Fig.10c). The SiO_2 versus AR [AR = $(Al_2O_3 + CaO + Na_2O + K_2O)/\ (Al_2O_3 + CaO + Na_2O - K_2O)$] binary diagram was devised by Middlemost (1994) to differentiate between peralkaline, alkaline, and calc-alkaline rock series. Plots of the analyzed granites on this diagram are shown in figure (10d). Most of the studied riebeckite- arfvedsonite granites are classified as peralkaline granites, meanwhile the biotite monzogranite and alkali feldspar granite classify as alkaline granites.

Trace elements have long been used to discriminate the different tectonic settings of granitic rocks. On the Nb versus Y diagram Pearce et al. (1984; Fig.10e), the studied granitic samples plot in the volcanic arc granite (VAG, I-type) field, whereas the studied riebeckite- arfvedsonite granites plot mainly in the field of within plate granites (WPG, A-type). According to Rb versus (Nb + Y) binary diagram of Pearce et al. (1984) proposed to differentiate between different tectonic settings of the granitic rocks. The plots of the analyzed granitic samples spread within different plate tectonic settings of volcanic-arc granites and within plate granites fields (Fig.10f).

Table 1. Chemical data (Major oxides, minor, and trace elements) of the study granitic rocks.

Rock place.	Gabal Gharib					Gabal Risays			Faliq El-Wa`ar		Wadi El-Ghafiryia				Wadi El- Ushsh		
Wt.%	**Peralkaline granites**					**Alkali feldspar granites**			**Biotite monzogranites**								
S. No.	1GG	2GG	5GG	7GG	10GG	1RS	3RS	4RS	2FW	4FW	1GH1	2GH1	3GH1	4GH1	2SH	3SH	4SH
SiO_2	69.48	72.14	72.03	70.89	72.71	66.59	63.94	65.87	73.20	73.10	69.75	67.64	69.12	67.81	63.31	62.61	62.72
TiO_2	0.30	0.17	0.17	0.26	0.19	0.39	1.04	0.44	0.11	0.31	0.43	0.41	0.42	0.44	0.84	0.84	0.84
Al_2O_3	14.07	13.32	12.86	13.69	13.01	16.74	14.67	16.85	14.09	14.15	15.03	14.37	14.53	14.77	16.51	16.05	16.24
FeO	1.36	1.10	1.20	1.37	1.19	0.86	2.36	1.07	0.46	0.44	1.15	1.08	1.09	1.13	2.11	2.06	2.07
Fe_2O_3	1.98	1.61	1.71	1.97	1.69	1.18	2.79	1.43	0.63	0.63	1.51	1.41	1.40	1.61	2.09	2.16	2.12
MnO	0.06	0.05	0.04	0.07	0.05	0.07	0.17	0.09	0.02	0.05	0.06	0.05	0.06	0.06	0.10	0.10	0.10
MgO	0.32	0.23	0.34	0.14	0.20	0.94	1.56	1.17	0.19	0.32	0.77	0.81	0.82	0.72	2.73	2.98	2.68
CaO	1.15	0.56	0.90	0.91	0.49	1.35	1.37	1.33	0.77	0.66	1.52	1.45	1.58	1.42	3.08	2.83	2.99
Na_2O	4.77	4.65	4.52	4.42	4.58	5.44	4.10	5.40	4.46	4.33	4.06	3.95	3.92	4.21	4.30	4.17	4.18
K2O	5.70	5.38	5.23	5.66	5.03	4.95	5.14	4.84	4.63	5.24	5.24	5.08	5.21	6.24	3.04	3.67	3.29
P_2O_5	0.05	0.03	0.04	0.05	0.01	0.13	0.41	0.16	0.03	0.04	0.19	0.18	0.20	0.21	0.33	0.38	0.40
SO3	0.03	0.01	0.01	0.02	0.03	0.06	0.02	0.03	0.04	0.17	0.08	0.25	0.75	0.29	0.18	0.28	0.08
Cl	0.08	0.03	0.04	0.03	0.03	0.05	0.03	0.03	0.03	0.04	0.04	0.06	0.03	0.17	0.05	0.04	0.08
LOI	0.55	0.30	0.60	0.31	0.51	0.57	0.41	0.57	0.50	0.47	0.13	3.22	0.66	0.83	1.20	1.70	2.11
Total	99.90	99.56	99.69	99.78	99.72	99.31	98.02	99.29	99.16	99.93	99.96	99.97	99.79	99.91	99.87	99.89	99.90
Sr	90	20	30	50	20	300	230	290	50	70	220	215	245	205	595	450	640
Zn	160	200	290	120	300	0	200	80	0	0	45	140	185	35	115	110	130
Ba	240	0	0	200	0	1560	1800	1690	480	150	810	1655	6400	585	740	1065	975
Ce	250	0	230	190	0	0	0	0	190	300	0	0	0	0	0	0	0
Co	0	0	0	0	0	0	18420	0	0	0	0	0	0	0	120	70	0
Cr	0	0	0	0	0	0	0	0	80	0	0	90	0	0	0	0	0
Cu	0	0	40	50	0	30	50	0	0	100	45	35	40	0	770	40	50
F	2440	5760	6010	0	5380	0	1260	0	0	0	0	0	0	0	0	0	0
Ga	40	60	70	50	70	30	50	20	30	30	0	0	0	0	0	0	0
Nb	170	170	320	110	280	10	20	20	10	20	0	0	0	0	0	0	0
Ni	0	40	40	40	0	0	50	40	30	40	0	0	0	0	0	0	0
Pb	0	40	50	20	30	60	20	40	30	60	0	0	0	0	0	0	0
Rb	260	420	470	180	440	140	150	120	150	160	0	0	0	0	0	0	0
Y	100	150	200	60	170	30	50	40	20	50	50	50	45	50	25	30	30
Zr	660	440	1100	670	1090	440	1550	510	200	500	470	465	490	485	470	385	450
Na_2O/K_2O	0.27	0.41	0.37	0.15	0.39	0.69	1.14	0.88	0.25	0.49	0.51	0.56	0.52	0.51	0.89	1.05	0.89

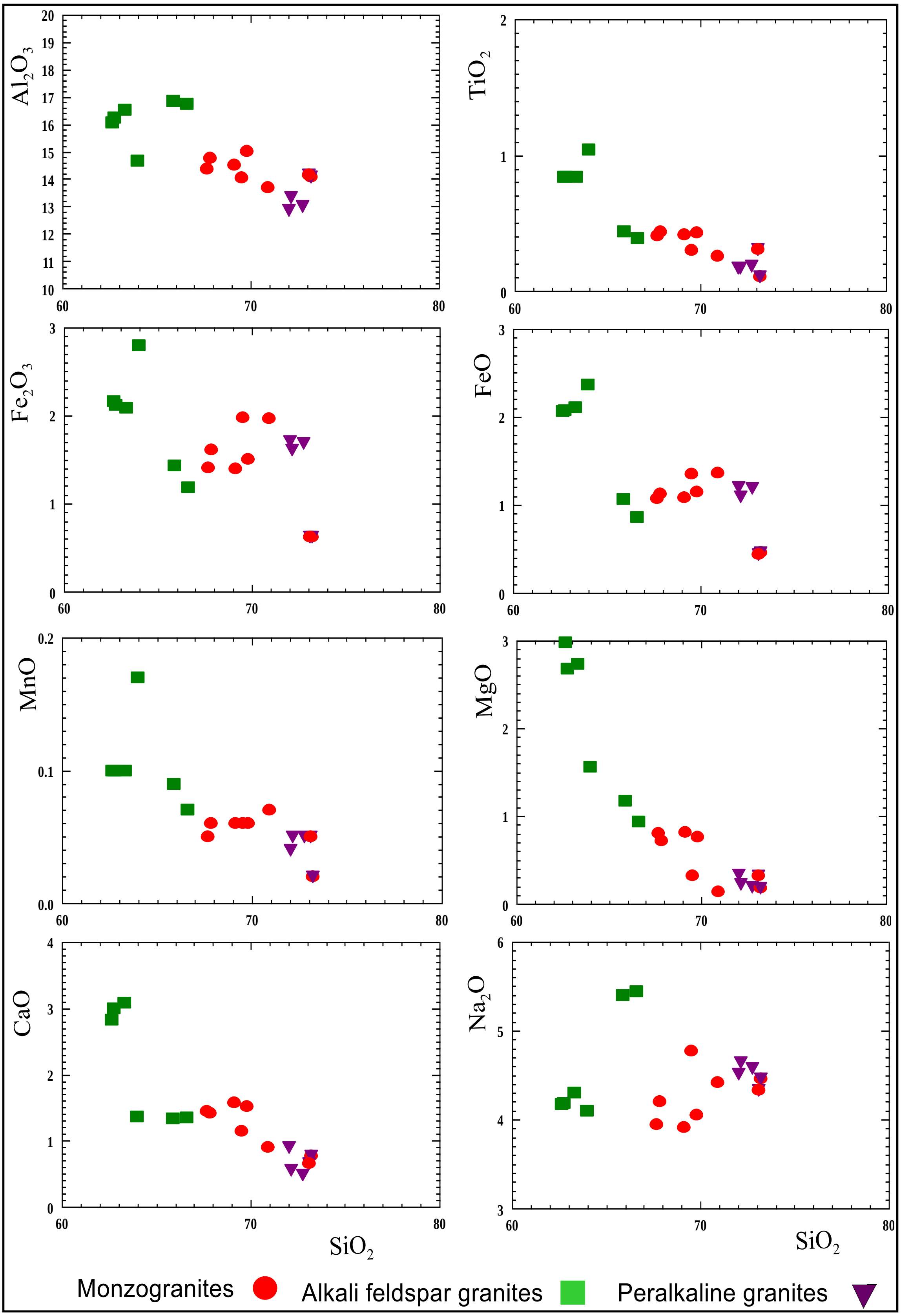

Fig. 8. Harker's variation diagrams (1909) of silica against major oxides of the granitic rocks.

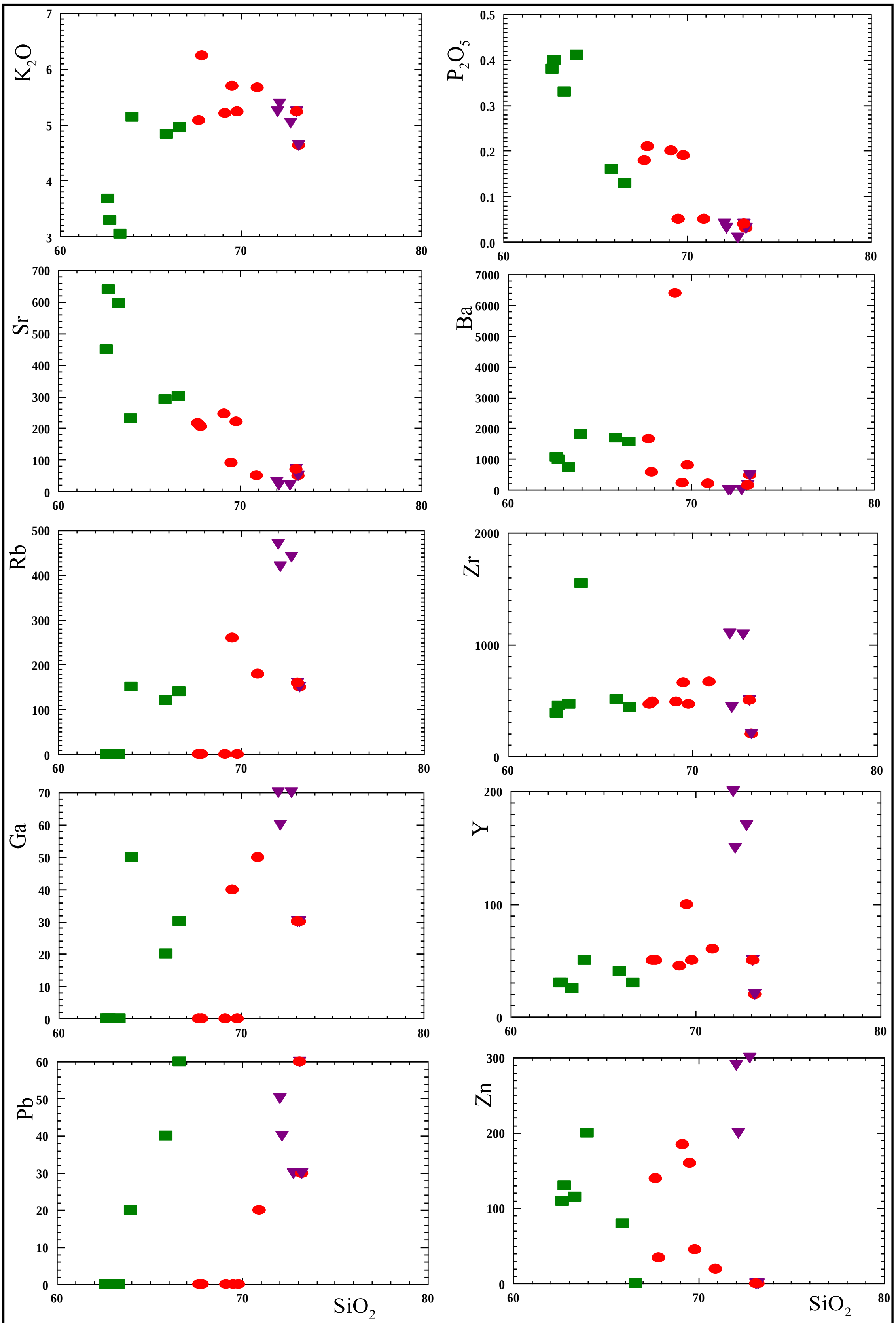

Fig. 9. Harker's variation diagrams (1909) of silica against some trace elements of the granitic rocks. Legend as in figure (8).

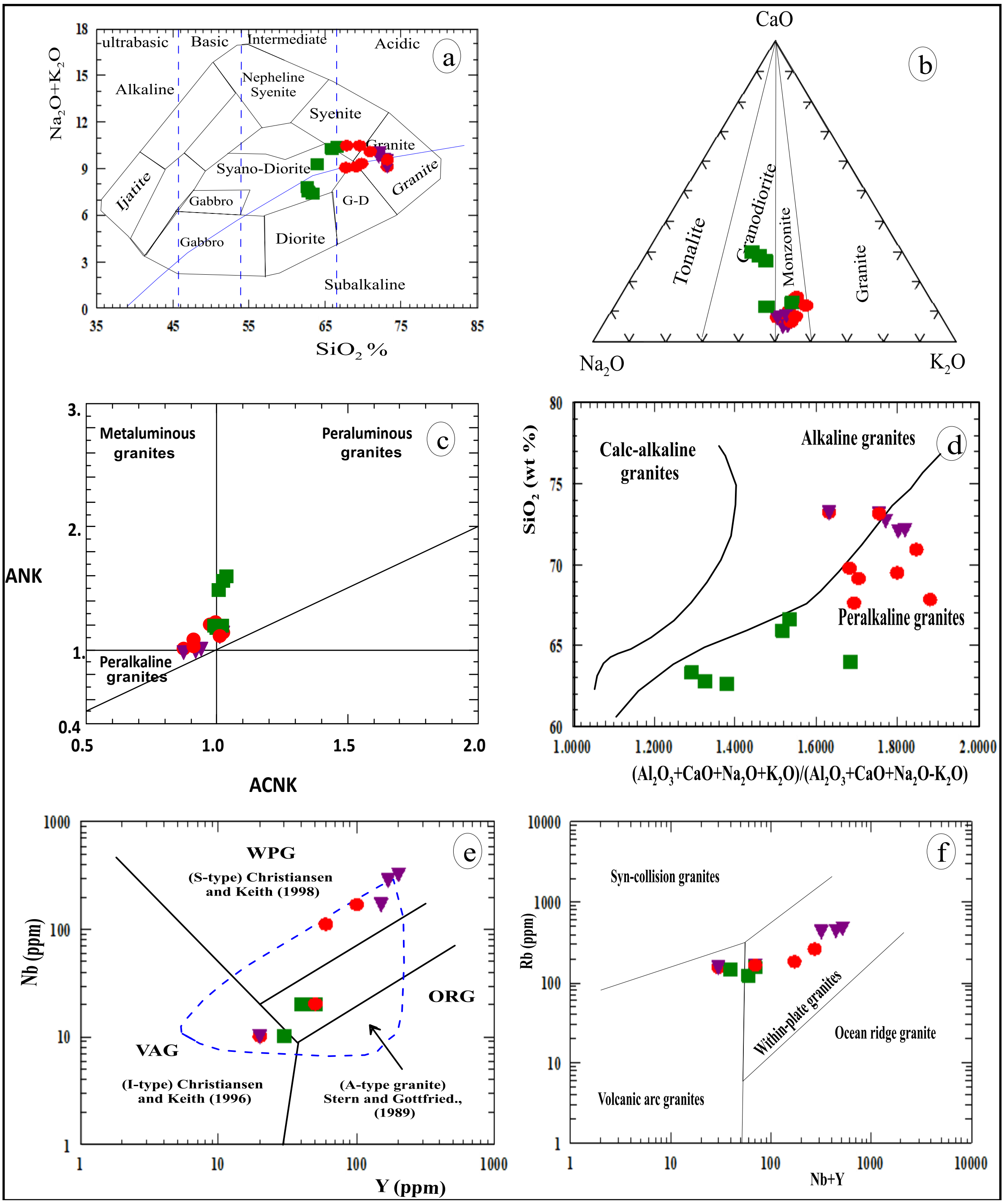

Fig. 10 (a-f). (a) SiO_2 versus (Na_2O+K_2O) variation diagram for the studied granitic rocks (Cox et al., 1979). (b) CaO - Na_2O - K_2O ternary diagram for the studied granitic rocks (Hunter et al., 1978). (c) ANK versus ACNK binary diagram of Maniar and Piccoli (1989) for the granitic rocks: A=Al_2O_3, C=CaO, N=Na_2O, and K=K_2O. (d) Plots of the analyzed granitic rocks on the SiO2 versus ($Al_2O_3 + CaO + Na_2O + K_2O$) /($Al_2O_3 + CaO + Na_2O–K_2O$) binary diagram (Middlemost, 1994). (e) Nb versus Y binary diagram after Pearce et al. (1984) for the studied granites; WPG: Within Plate Granitoids; COLG: Collision Granitoids; ORG: Orogenic Related Granitoids; VAG: Volcanic Arc Granitoids. (f) Rb versus Nb + Y binary diagram of Pearce et al. (1984) for the studied granites. Legend as in figure (8).

3.3 Purpose and Scope of Mechanical and Physical Investigation

Rocks show a variety of physical and mechanical properties that may affect the use of rocks as a construction material, they are widely used in structural and constructional works, and the physical and mechanical properties are functions of mineralogical and textural characteristics of rock (Irfan, 1996). Those properties also may affect quarrying operation, tunneling mining slope stability and the use of rock as constructional material (Tugrul and Zarif, 1999).

The experiments aimed to investigate the fundamental physical and mechanical properties of the studied granite specimens. The following tests are examples of the mechanical and physical characteristics that were found during this study: Compressive strength, water absorption, apparent porosity, thermal expansion, and abrasion resistance.

3.3.1 Compressive strength

The compressive strength test was applied in displacement control mode until the sample reached its point of failure under conventional uniaxial compression ASTM C 170 – 99: Standard Test Method for Compressive Strength of Dimension Stone. Compressive strength is one of the basic parameters, which use to detect the quality of natural ornamental stones. Compressive strength may be defined as a material's ability to withstand loads that tend to shrink size or as its resistance to rupturing under pressure from forces operating on a rock sample from both above and below.

The relationships between uniaxial compressive strength of the ornamental stones and their physical properties were studied by Scott and Nielson (1991) and Palchik and Hatzor (2000). The results of compressive strength of the studied granitic samples are showing in Figures (11 & 15a) and table (3).

The results of the compressive strength for the studied granitic samples are as follows: Wadi Faliq El-Wa`ar granites ranges from 818 to 850 kg/cm^2 with an average 836 kg/cm^2; Wadi El-Ghafiryia granites ranges from 910 to 938 kg/cm^2 with an average 926 kg/cm^2; Wadi Al-Ushsh granites ranges from 783 to 810 kg/cm^2 with an average 795 kg/cm^2, Gabal Risays granites (1) ranges from 927 to 947 kg/cm^2 with an average 938 kg/cm^2, Gabal Risays granites (2) ranges from 914 to 923 kg/cm^2 with an average 917 kg/cm^2, Gabal Gharib granites (1) ranges from 960 to 995 kg/cm^2 with an average 979 kg/cm^2, and Gabal Gharib granites (2) ranges from 948 to 972 kg/cm^2 with an average 958 kg/cm^2. The lowest values of the compressive strength are recorded in Wadi Al-Ushsh granites (795), meanwhile the highest values are recorded in Gabal Gharib granites (1), ((979 kg/cm^2; table 3).

3.3.2 Apparent porosity

It is the proportion between the exterior volume and the size of the connecting pore space in the rock. It utilized to provide a thorough understanding of compressive strength, weather resistance, and frost resistance. The factors affecting rock porosity include grain size, grain shape, and mineral composition, especially clay minerals (Bell, 1978). The obvious porosity is mostly less than 0.6 %. Generally, the porosity of ornamental stone is more than 0.6%, require extra caution if utilized for outside work. Increased porosity negatively affects the properties of weathering. (Ruedrich et al., 2010).

Calculated formula: -

Apparent Porosity (%) = {(B-A)/(B-C)} *100

Where: A = Weight of oven-dry test sample (g).

B = weight of saturated-surface-dry test sample (g).

C = weight of saturated test sample in water (g).

The results of the apparent porosity for the studied granitic rocks are as follows: Wadi Faliq El-Wa`ar granites ranges from 0.54 to 0.54% with an average 0.54%; Wadi El-Ghafiryia granites ranges from 0.50 to 0.50% with an average 0.50%; Wadi Al-Ushsh granites ranges from 0.50 to 0.62% with an average 0.56%; Gabal Risays granites (1) ranges from 0.34 to 0.76% with an average 0.52%; Gabal Risays granites (2) ranges from 0.41 to 0.70% with an average 0.53%; Gabal Gharib granites (1) ranges from 0.22 to 0.79% with an average 0.46%; and Gabal Gharib granites (2) ranges from 0.23 to 0.41% with an average 0.34% as show in Table (3) and Figure (15f).

The relationship between compressive strength and apparent porosity of the studied granitic samples exhibits reversible relation as show in Figure (11), where the compressive strength decreases with the inter pore space increase, but the results of apparent porosity for these granitic rocks is mostly less than 0.6% so that it is suitable for outdoor work.

3.3.3 Specific gravity

It is represented by the real proportion between the bulk density of the rock material and the bulk density of water at 4°C ASTM C 97-02: Test Methods for Absorption and Bulk Specific Gravity of Dimension Stone. Specific gravity of the investigated granitic samples was detected and the results are found in table (3).

Calculated formula:

Specific gravity: A/(A-C).

Where: A = Weight of oven-dry test sample (g).

B: Weight of saturated-surface-dry test sample in air (g).

C = Weight of saturated test sample in water (g).

The results of the specific gravity for Wadi Faliq El-Wa`ar granites ranges from 2.70 to 2.70 with an average 2.70; Wadi El-Ghafiryia granites ranges from 2.74 to 2.74 with an average 2.74; Wadi Al-Ushsh granites ranges from 2.67 to 2.67 with an average 2.67; Gabal Risays granites (1) ranges from 2.72 to 2.73 with an average 2.73; Gabal Risays granites (2) ranges from 2.71 to 2.72 with an average 2.71; Gabal Gharib granites (1) ranges from 2.79 to 2.80 with an average 2.79; and Gabal Gharib granites (2) ranges from 2.75 to 2.76 with an average 2.76 (Fig.15c), all results ≥ 2.5. These results are appropriate with heavy construction works (Blyth and De Freitas, 2017).

The examined granitic samples' compressive strength and bulk specific gravity show an irreversible link as show in Figure (12), where the compressive strength increases with the increasing of bulk specific gravity and observed specific gravity of the studied granitic samples that refers to their suitability for used as ornamental stone in the construction projects.

3.3.4 Water absorption

Water absorption was used to investigate the pores in the rock and the connectivity of the micro fissures. It is a main property in assessing rock durability, which using as building materials (Shakoor and Bonelli, 1991). Water absorption is the increase in the weight of stone due to water in the pore spaces of the materials, but not including water adhering to the outside surface of the particles, expressed as a percentage of the dry weight. The water absorption results are found in Table (3) showing low content less than 1%.

Calculated formula: -

Water Absorption % = {(A-B)/A} *100

Where: A: Weight of oven-dry test sample (g).

B: Weight of saturated-surface-dry test sample (g).

The results of water absorption are as follows: Wadi Faliq El-Wa`ar ranges from 0.20 to 0.20% with an average 0.20%; Wadi El-Ghafiryia ranges from 0.18 to 0.18% with an average 0.18 %; Wadi Al-Ushsh ranges from 0.19 to 0.23% with an average 0.213%; Gabal Risays (1) ranges from 0.13 to 0.28% with an average 0.192 %; Gabal Risays (2) ranges from 0.15 to 0.26% with an average 0.196; Gabal Gharib (1) ranges from 0.08 to 0.29% with an average 0.164%; and Gabal Gharib (2) ranges from 0.08 to 0.1 % with an average 0.125% (Fig.15b).

The relationship between compressive strength and water absorption of the studied granitic samples exhibits reversible relation as show in Figure (14), whereas the compressive strength decreases with increase the ability of granitic rocks to passing water through it. Meanwhile The granitic samples under study exhibit a water absorption of less than 1% by weight and possess great weather resilience, making them suitable for use as dimensional stones (Blyth and De Freitas, 2017).

3.3.5 Abrasion resistance

Abrasive resistance is a measure of a rock's hardness and the amount of granitic rocks that can withstand abrasion without suffering damage based on the durability and quality of the rock. in addition to good results for some physical and mechanical properties such as apparent porosity and compressive strength tests. The studied granitic samples have good results (Table 5) according to standard values of Bates (1969), Brown (2015) and ASTM C 241-90 (2005).

3.3.6 Thermal expansion

An essential property for characterizing dimensional stones is thermal expansion. Granitic samples under investigation were heated to high temperatures in convection ovens; as a result, the material's linear dimensions gradually increased. The thermal expansion values of the studied granitic samples are match with the international standard of the ornamental stones. The results of thermal expansion values for Wadi Faliq El-Wa`ar granites ranges from 0.03 to 0.05cm with an average 0.040cm; Wadi El-Ghafiryia granites ranges from 0.045 to 0.055cm with an average 0.050cm; Wadi Al-Ushsh granites ranges from 0.050 to 0.070cm with an average 0.058cm; Gabal Risays granites (1) ranges from 0.03 to 0.045cm with an average 0.037 cm; Gabal Risays granites (2) ranges from 0.04 to 0.04cm with an average 0.04 cm; Gabal Gharib granites (1) ranges from 0.015 to 0.025cm with an average 0.020cm; and Gabal Gharib granites (2) ranges from 0.015 to 0.035 cm with an average 0.025cm (Table 2 and Fig.15d) according to Bates (1969) and Brown (2015). The relationship between the compressive strength and thermal expansion of the studied granitic samples exhibits reversible relation (Fig.13), where the compressive strength decreases with increase the ability of granitic rocks to expansion.

Table 2. Shows the physical requirements for assessment the studied granitic rocks for building purpose.

Physical Property	Physical Property	Test Method (s)
Absorption by weight, max, %	0.40	C 97
Density, min, l b /ft3 (kg/m^3)	160 (2560)	C 97
Compressive strength, min, psi (MPa)	19 000 (131)	C 170
Modulus of rupture, min, psi (MPa)	1500 (10.34)	C 99
Abrasion resistance, min, Ha A, B, C	25	C 241/C 1353
Flexural strength, min, psi (MPa)	1200 (8.27)	C 880

3.3.7 Acid resistance

It is identified by observing how sulfuric and hydrochloric acids react with granite materials for an hour. The granite samples under study provide good results in terms of acid resistance (Table 4). Therefore, the studied granitic rocks are considered to have great economic value in the manufacture of ornamental stones and building materials.

3.3.8 Weather and frost

Weather and frost are the resistances of weathering degree generally expressed in terms of changes in the physical and mechanical properties of the rock material. Beavis (1985) suggested some important and main points that should be considered when determining weathering degree as follows: -

1. Changes in color and texture of rock material and rock mass.
2. Changes in strength (uniaxial compressive strength, point load strength etc.).
3. Changes in porosity of rock material.
4. Determination of Rock Quality Designation (RQD).

The studied samples have been placed in water, dried their surface from the water and stored in room that has very low temperature (less than 0 ºC) for more than four weeks nearly. The granitic samples under study exhibited strong resistance to fragmentation and corrosion. Additionally, they are resistant to frost and weathering well. according to measured values abrasion, weather, frost, and acid resistance (Table 5).

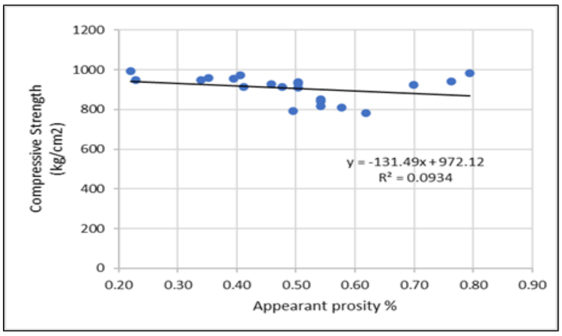

Fig. 11. shows the compressive strength versus apparent porosity of the studied granitic samples.

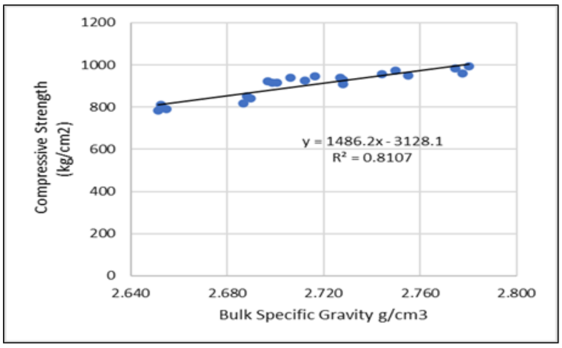

Fig. 12. shows the compressive strength versus bulk specific gravity of the studied granitic samples.

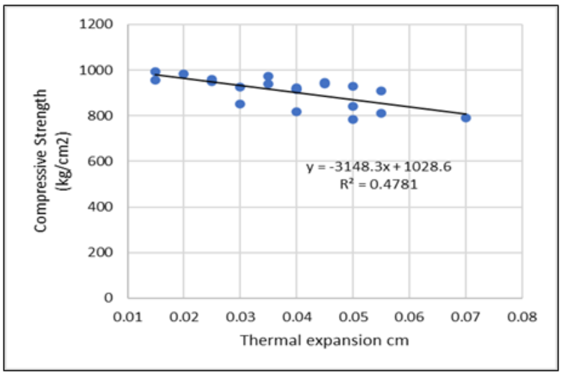

Fig. 13. shows the compressive strength versus thermal expansion of the studied granitic samples.

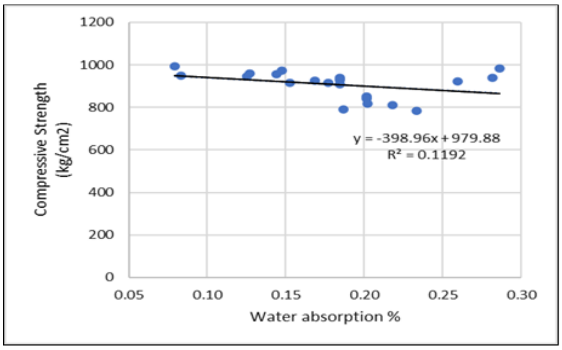

Fig. 14. shows the compressive strength versus water absorption for the studied granitic samples.

Table 3. The mechanical and physical properties of the studied granitic samples.

S. No.	Apparent specific gravity	Bulk specific gravity (g/cm^3)	Water absorption (%)	Apparent porosity (%)	Compressive strength (kg/cm^2)	Thermal expansion (cm)
FW	2.70	2.69	0.20	0.54	850	0.03
	2.70	2.69	0.20	0.54	840	0.05
	2.70	2.69	0.20	0.54	818	0.04
Gh1	2.74	2.73	0.18	0.50	930	0.05
	2.74	2.73	0.18	0.50	938	0.045
	2.74	2.73	0.18	0.50	910	0.055
Sh	2.67	2.65	0.22	0.58	810	0.055
	2.67	2.65	0.23	0.62	783	0.05
	2.67	2.65	0.19	0.50	792	0.07
Rs1	2.72	2.71	0.17	0.46	927	0.03
	2.73	2.72	0.13	0.34	947	0.045
	2.73	2.71	0.28	0.76	941	0.035
Rs2	2.71	2.70	0.18	0.48	915	0.04
	2.72	2.70	0.26	0.70	923	0.04
	2.71	2.70	0.15	0.41	914	0.04
GG1	2.79	2.78	0.13	0.35	960	0.025
	2.80	2.77	0.29	0.79	982	0.02
	2.79	2.78	0.08	0.22	995	0.015
GG2	2.76	2.75	0.15	0.41	972	0.035
	2.75	2.74	0.14	0.40	955	0.015
	2.76	2.76	0.08	0.23	948	0.025

Table 4. The average mechanical and physical properties of the studied granitic samples.

S. No.	Apparent Specific Gravity	Bulk specific gravity (g/cm^3)	Water absorption (%)	Apparent porosity (%)	Compressive strength (kg/cm^2)	Thermal expansion (cm)
FW	2.7	2.688	0.20	0.542	836	0.040
Gh1	2.74	2.728	0.18	0.504	926	0.050
Sh	2.668	2.653	0.213	0.56	795	0.058
Rs1	2.726	2.712	0.192	0.52	938	0.037
Rs2	2.713	2.699	0.196	0.53	917	0.040
GG1	2.790	2.778	0.164	0.46	979	0.020
GG2	2.759	2.750	0.125	0.34	958	0.025

Fig. 15 (a-f). showing the samples numbers versus each of compressive strength (a), water absorption (b), apparent specific gravity (c), thermal expansion (d), bulk specific gravity (e), and apparent porosity (f) for the studied granitic rocks.

Table 5. The abrasion, weather, frost, and acid resistance of the studied granitic samples.

S. No.	Abrasion resistance	Weather and frost resistance	Acid resistance (HCl & H_2SO_4)
FW	Good	Good	Good
Gh1	Good	Good	Good
Sh1	Good	Good	Good
Rs1	Good	Good	Good
Rs2	Good	Good	Good
GG1	Good	Good	Good
GG2	Good	Good	Good

RS1= Gabal Risays location 1; FW= Wadi Faliq El-Wa`ar; Gh1= Wadi El-Ghafiryia; RS2= Gabal Risays location 2; Sh1= Wadi Al-Ushsh; GG1= Gabal Gharib location 1; GG2= Gabal Gharib location 2.

4. Conclusion

The studied area is located in the northeastern Desert of Egypt ranges from medium to high mountainous terrain exposed at Gabal Risays and Gabal Gharib. This area is traversed by a number of wadis flowing north-east towards the Gulf of Suez, such as Wadi Faliq El-Wa`ar, Wadi El-Ghafiryia, and Wadi Al-Ushsh. The studied granites are represented by late-orogenic granites (Monzogranites and alkali feldspar granites) and post-orogenic granites (Peralkaline granites). Several post-orogenic dykes with a basic composition cut through the granitic rocks under investigation. Monzogranites are buff in color, medium to coarse-grained and characterized by low to moderate relief, jointed, bouldery weathering, and spheroidal exfoliation exposed at Wadi Falig El-Wa`ar.

Petrographically, the studied granites are represented by biotite monzogranites, alkali feldspar granites, and riebeckite-arfvedsonite granites. These granites are medium-grained and consist essentially of quartz, K-feldspars, albite with subordinate amounts of biotite and quartz. Biotite monzogranite is composed essentially of quartz, perthite, plagioclase, potash feldspar (Microcline and orthoclase), and biotite as well as opaques, allanite, zircon, apatite, and titanite are accessories. Chlorite, kaolinite, and sericite occur as secondary alteration minerals. Alkali feldspar granite consists essentially of quartz, potash feldspars, plagioclase, and orthoclase perthite crystals. They are medium- to coarse-grained, euhedral to subhedral crystals and showing often perthitic texture. Riebeckite - arfvedsonite granites is composed mainly of alkali feldspars with interstitial quartz, arfvedsonite, and riebeckite.

The granitic rocks are classified by using several diagrams as the granite, granodiorite, syenodiorite, monzonite, syenite, and alkali granite fields. These granites show wide variation of the examined biotite monzogranite and alkali feldspar granite samples, where they are lying on the field of metaluminous to peraluminous orogenic I-type granites. Meanwhile, the riebeckite- arfvedsonite granite samples are metaluminous to peralkaline anorogenic A-type granites. The most of studied riebeckite-arfvedsonite granites are classified as peralkaline granites; meanwhile the biotite monzogranite and alkali feldspar granite classified as alkaline granites.

Microstructure of ornamental stones plays a major role in its behavior of physical and mechanical properties. The mineral composition and petrographic characteristics of the examined granites, such as deformation processes that resulted development of plans of weakness, and consequently, facilitated the alteration processes. appeared to have an impact on the granites' physicomechanical properties. So that when the apparent porosity, water absorption, and thermal expansion increase as result to microstructure of ornamental stones tend to the compressive strength decrease but with increasing the bulk specific gravity and apparent specific gravity as a function of the amount of iron-rich minerals, quartz, and feldspars content tend to increase the compressive strength.

Granite is a common type of rock in underground rock engineering because it's high strength and low permeability. Because they may be used, granitic rocks with eye-catching hues and a high degree of hardness are highly valuable economically as decorative stones and construction in addition to various industrial purposes. The results of physical and mechanical properties of the studied granitic rocks revealed that the average of compressive strength ranges from 795 kg/cm2 (Wadi Al-Ushsh) to 971 kg/cm2 (Gabal Gharib). The maximum water absorption values are of (0.22 %) for Wadi Al-Ushsh granites. Meanwhile, the lowest values of water absorption is (0.13 %) for Gabal Gharib granites. The apparent specific gravity of the studied granitic rocks ranges from 2.67 to 2.79 gm/cm3 with average 2.73 gm/cm3. The studied granitic samples have a good result of mechanical and physical tests. So that it can be used in decoration purposes and construction materials.

5. References

Agasnalli, C., Hema, H.C., Lakkundi, T., Chandrappa, K.D. (2022). Integrated assessment of granite and basalt rocks as building materials. *Materials Today: Proceedings*, **62**, 5388-539. DOI: 10.1016/j.matpr.2022.03.546

Akaad, M.K., El-Gaby, S., Habib, M.E. (1973). The Barud gneisses and the origin of grey granite. *Bull. Fac. Sci. Assiut Univ*., **2**, 55-69.

ASTM C 241-90 (2005) Standard test method for abrasion resistance of stone subjected to foot traffic

Awad, H.A., Zakaly, H.M., Nastavkin, A.V., El-Taher, A. (2022). Radioactive content and radiological implication in granitic rocks by geochemical data and radiophysical factors, Central Eastern Desert, Egypt. *International Journal of Environmental Analytical Chemistry*, **102**(19), 7444-7457. DOI: 10.1080/03067319.2020.1830987

Bates, R.L. (1969). Geology of the industrial rocks and minerals. *Dover Pubns; 2nd edi* **460** pp.

Beavis, F.C. (1985). Rock Weathering. In: Engineering Geology. *Blackwell Scientific, Melbourne*. pp 52-91.

Bell, F.G. (1978). The physical and mechanical properties of the fell sandstones, Northumberland, England. *Engineering Geology*, **12**, 1-29.

Blyth, F.G.H., De Freitas, M. (2017). A geology for engineers. *7th ed. CRC Press*.

Brown, E.T. (2015). Rock engineering design of post-tensioned anchors for dams–a review. *Journal of rock mechanics and geotechnical engineering,* **7**(1), 1-13. DOI: 10.1016/j.jrmge.2014.08.001

Ciccu, R., Cosentino, R., Montani, C., El-Kotb, A., Hamdy, H. (2005). "Strategic study on the Egyptian marble and granite sector," *Ind. Mod. Cent. (IMC),* Cairo,

Cox, K.G., Bell, J.D., Ponkhurst, R.J. (1979). The interpretation of igneous rocks. *George Allen and Unwir*, London.

Dino, G.A., Passarella, I., Ajmone-Marsan, F. (2015). Quarry rehabilitation employing treated residual sludge from dimension stone working plant. *Environmental Earth Sciences*, **73**, 7157-7164.

El-Gaby, S., Habib, M.S. (1982). Geology of the area southwest of Port Safaga, with special emphasis on the granitic rocks, Eastern Desert, Egypt.

El-Bialy, M.Z., Omar, M. M. (2015). Spatial association of Neoproterozoic continental arc I-type and post-collision A-type granitoids in the Arabian–Nubian Shield: the Wadi Al-Baroud older and younger granites, north eastern desert, Egypt. *Journal of African Earth Sciences*, **103**, 1-29. DOI: 10.1016/j.jafrearsci.2014.11.013

El-Desoky, H., Abd El-Hafez, N., Khalil, A., Arafat, A., Hasan, M., Youssef, T. (2023). The Geology, Petrography, and Geochemistry of Egyptian Dokhan Volcanics: A Potential Source for Construction Aggregate. *Minerals*, 13(5), **635**. DOI: https://doi.org/10.3390/min13050635

El-Gaby, S., (1990) "The basement complex of the Eastern Desert and Sinai," *Geol. Egypt*, pp. 175–184.

Habib, M.E. (1987). Microplate accretion model for the Pan-African basement between Qena-Safaga and Qift-Quseir roads, Egypt. *Bulletin of the Faculty of science. Assiut university. C. Biology and geology,* **16**(1), 199-239.

Harker, A., (1909). The natural history of igneous rocks, *Macmillan, New York,* **384**pp

Harrell, J.A. (2013). Ornamental stones. *UCLA Encyclopedia of Egyptology*, **1**(1). DOI: https://escholarship.org/uc/item/4xk4h68c

Hassan, M.A., Hashad, A.H., (1990). Pre-Cambrian Egypt. In: Said, R. (ed.), Geology of Egypt. *Balkema Publications, Netherlands,* **734** pp.

Hunter, D.R., Barker, F., Millard, H. T. (1978). The geochemical nature of the Archaean ancient gneiss complex and granodiorite suite, Swizerland: *A prelimnary study. Precambrian Res*. **7**, 105-127

Irfan, T.Y. (1996). Mineralogy, Fabric Properties and Classification of Weathered Granites in Hong Kong. *Quarterly Journal of Engineering Geology*, No. **29**, p. 5-35.

Jarrar, G., Stern, R. J., Saffarini, G., Al-Zubi, H. (2003). Late-and post-orogenic Neoproterozoic intrusions of Jordan: implications for crustal growth in the northernmost segment of the East African Orogen. *Precambrian research*, **123**(2-4), 295-319. DOI: https://doi.org/10.1016/S0301-9268(03)00073-1

Maniar, P.D., Piccoli, P.M. (1989). Tectonic discrimination of granitoids. *Geological society of America bulletin*, **101**(5), 635-643.

Middlemost, E.A.K. (1994). Naming materials in the magma/igneous rock system. *Earth-science reviews*, **37**(3-4), 215-224.

Moghazi, A.M., (2003). Geochemistry and petrogenesis of a high-K calc-alkaline Dokhan volcanic suite, South Safaga area, Egypt: the role of late Neoproterozoic crustal extension. *Precambrian Res*. **125**, 161–178. DOI: https://doi.org/10.1016/S0301-9268(03)00110-4

Noweir, A.M., Sewifi, B.M., Abu El-Ela, A.M. (1990). Geology, petrography, geochemistry and petrogenesis of the Egyptian younger granites. *Qatar University Science Bulletin* **10**, 363–393.

Palchik, V., Hatzor, Y.H., (2000). Correlation between mechanical strength and microstructure parameters of dolomite and limestone in the Judea group‖, Israel Isr. J. *Earth Sci*. **49** (2), 65-79.

Pearce, J.A., Harris, N.B., Tindle, A.G. (1984). Trace element discrimination diagrams for the tectonic interpretation of granitic rocks. *Journal of petrology*, **25**(4), 956-983.

Ramly, E. (1972). A new geological map for the basement rocks in the Eastern and Southwestern Deserts of Egypt. *Ann. Geol. Survey of Egypt*, **2**, 1.

Ruedrich, J., Bartelsen, T., Dohrmann, R., Siegesmund, S. (2010). Building sandstone integrity affected by the process of hygric expansion. *Environ Earth Sci*. doi, **10**.

Scott, T.E., Nielson, K.C. (1991). The effect of porosity on brittle– ductile transition in sandstones, *J. Geophys. Res*. **96**, pp. 405– 414.

Shakoor, A., Bonelli, R.E. (1991). Relationship between petrographic characteristics, engineering index properties, and mechanical properties of selected sandstones. *Bulletin of the Association of Engineering Geologists*, **28**(1), 55-71.

Stern, R.J. (1979). Late Precambrian ensimatic volcanism in the central Eastern Desert of Egypt. *Unpublished Ph.D. Thesis, University of California, San Diego*.

Stern, R.J., Gottfried, D. (1986). Petrogenesis of late Precambrian (575– 600 Ma) bimodal suite in north-east Africa. *Contributions to Mineralogy and Petrology* **92**, 492–501.

Stern, R.J., Hedge, C.E. (1985). Geochronological and isotopic constraints on the Late Precambrian crustal evolution in the Eastern Desert of Egypt. *Am. J. Sci*. **285**, 97-12.

Shahin, T.M. (2023). Petrogenesis and Geochemical Implications of Neoproterozoic Gabal Ras Zeraib Granites, Central Eastern Desert, Egypt. *Dokl. Earth Sc.* **512**, 983–997. https://doi.org/10.1134/S1028334X23600421

Tuğrul, A., & Zarif, I. H. (1999). Correlation of mineralogical and textural characteristics with engineering properties of selected granitic rocks from Turkey. *Engineering geology,* **51**(4), 303-317.

Willis, K.M., Stern, R.J., Clauer, N. (1988). Age and geochemistry of Late Precambrian sediments of the Hammamat Series from the Northeastern Desert of Egypt. *Precambrian Research,* **42**(1-2), 173-187.

بترولوجية وجيوكيمياء بعض الصخور الجرانيتية المصرية: تقييم الخواص الفيزيائية والميكانيكية للجرانيت المستخدم كمواد بناء

أحمدعرفات [١]، وحاتم الدسوقي[١]، ونبيل عبدالحافظ [١]، وأحمد خليل [٢]

[١] قسم الجيولوجيا، كلية العلوم، جامعة الأزهر، ص.ب ١١٨٨٤، مدينة نصر، القاهرة، مصر

[٢] قسم الجيولوجيا، المركز القومي للبحوث، الدقي، القاهرة، مصر

تتناول الدراسة الحالية الجيولوجيا الحقلية والبتروجرافية والجيوكيميائية لبعض الصخور الجرانيتية المصرية ومدى ملاءمتها لمواد البناء. كما يهدف العمل الحالي إلى تحديد الخواص الفيزيائية والميكانيكية لبعض الجرانيت في شمال الصحراء الشرقية مصر للكشف عن مدى ملاءمتها لأحجار الزينة. تعتبر الصخور الجرانيتية من أهم السلع التجارية وتستخدم في مجموعة متنوعة من الاستخدامات، بما في ذلك أحجار الزينة.

تتكون منطقة الدراسة جيولوجياً من تلال جبلية متوسطة الارتفاع ذات تضاريس صلبة وقمم متعرجة. وقد تم تصنيف العينات التي تم جمعها من الناحية البتروجرافية إلى البيوتيت مونزوجرانيت، وجرانيت الفلسبار القلوي، وجرانيت الريبكيت–أرففيدسونيت (جرانيت بيرالكالاين). وفي الوقت نفسه، تم تصنيفها كيميائيا إلى مونزوجرانيت وجرانيت الفلسبار القلوي وجرانيت البيرالكالين.

الاختبارات التطبيقية الرئيسة للخصائص الفيزيائية والميكانيكية تشمل مقاومة الضغط، المسامية الظاهرة، الثقل النوعي، إمتصاص الماء، التمدد الحراري، مقاومة التآكل والطقس والصقيع والأحماض. تم تقطيع العينات المدروسة حسب مواصفات الجمعية الأمريكية للاختبارات والمواد (الشكل المكعب) للكشف عن الخواص الفيزيائية والميكانيكية وهى كالتالى تتراوح قوة الضغط من ٧٩٥ إلى ٩٧٩ كجم / سم^{٣}، وتتراوح المسامية الظاهرية من ٠,٣٥٪ إلى ٠,٥٨٪، وتتراوح الثقل النوعي من ٢,٦٧ إلى ٢,٧٩ جم / سم^{٢}، ويتراوح امتصاص الماء من ٠,١٣٪ إلى ٠,٢٢٪، والتمدد الحراري تتراوح من ٠,٠٢ إلى ٠,٠٦، ومقاومتها للتآكل وظروف الطقس والصقيع والأحماض جيدة،. تجدر الإشارة إلى أن عينات الجرانيت المدروسة أظهرت نتائج جيدة حسب الاختبارات الميكانيكية والفيزيائية. بحيث يمكن استخدامه في أغراض الديكور ومواد البناء.